

## Research Article

# Mechanical Mechanism of Water Injection to Enhance the Stability of Soft Coal

Chuanqi Zhu <sup>1</sup>, Hao Fan <sup>1</sup>, Wanrong Liu,<sup>1,2</sup> and Shaobo Li <sup>1</sup>

<sup>1</sup>State Key Laboratory of Mining Response and Disaster Prevention and Control in Deep Coal Mines, Anhui University of Science and Technology, Huainan 232001, China

<sup>2</sup>School of Architecture & Civil Engineering, Liaocheng University, Liaocheng, Shandong 252059, China

Correspondence should be addressed to Hao Fan; fanhao2014@126.com

Received 4 August 2021; Accepted 3 September 2021; Published 14 September 2021

Academic Editor: Zhengyang Song

Copyright © 2021 Chuanqi Zhu et al. This is an open access article distributed under the Creative Commons Attribution License, which permits unrestricted use, distribution, and reproduction in any medium, provided the original work is properly cited.

The physical and mechanical properties of soft coal body constitute one of the most important factors inducing coal wall spalling. In order to explore the mechanical essence of coal instability disaster and stability enhancement of water injection, the 7<sup>#</sup> coal in Huainan mining area is taken as the research object. Firstly, the distribution characteristics of coal particle size, point-load strength, original water content, microstructure characteristics, and shear strength of coal under different water contents are measured by laboratory tests. Then, based on the test results, the cementation morphology and force evolution law of granular coal water in coal body are analyzed using liquid bridge theory. The results show the following: (1) With the increase of particle size, the mass ratio of granular coal increases gradually. The percentage of particle coal with particle size less than 2.5 mm accounts for 47.157%, fractal dimension is 2.172, and uniaxial compressive strength and tensile strength are 3.822 MPa and 0.165 MPa, respectively. (2) The coal body is dry (the original moisture content is 1.336%), containing a large number of loose particles, pores, fissures, and other microfibrils. This “low water content and multiporosity” feature is the essential reason for its low strength, fragmentation, and instability and disaster. (3) In the process of water content increasing from 0.966% to 26.580%, the shear stress-displacement curve of coal body gradually changes from softening type to hardening type, and the failure type transitions from brittleness to ductility. The cohesive force increases first and then decreases, while the angle of internal friction almost has no change. (4) After reasonable water injection, the shape of liquid bridge in coal body changes into capillary tube, and the liquid bridge force reaches the maximum value, which transforms from a highly unstable bulk to a stable continuum. The research results have important theoretical significance and practical value for the safe and efficient mining of soft coal seams.

## 1. Introduction

Coal slip and roof fall often occur when mining the work face with large heights, large inclination angles, and soft coal seams, which seriously affect the mining efficiency, cause economic losses, and threaten human safety. In order to control the stability of the surrounding rock of the working face, a lot of research on the characteristics and control techniques of instability of coal wall have been carried out. Wang et al. [1], Xu et al. [2], and Pang et al. [3] found that the plastic failure zone in front of the coal wall in the high-cutting fully mechanized caving mining is obviously greater than that of the large-cutting fully mechanized mining. A suitable protective plate structure and a reasonable

protective method are proposed by analyzing the characteristics of coal wall slabs in the working face with super large mining height. Zhang [4] established a mechanical model for analyzing the slab side of the coal wall in a fully mechanized caving face with large mining height in extra-thick coal seams and revealed the mechanical mechanism of the slab side. Based on the main influencing factors of the flanks, reasonably determining the height of the machine mining, appropriately increasing the advance speed, and determining a reasonable coal cutting speed were put forward to prevent coal siding. Li et al. [5] established a mechanical model of the coal wall sliding slab and judged the stability of the coal body on the sliding surface. Jin et al. [6] established a cusp catastrophe model of coal wall instability and analyzed

the conditions of the slabs. Reducing the pressure on the coal wall, making full use of the protection board, and strengthening the coal wall were proposed to prevent coal siding. Wu et al. [7] researched the mechanism of coal wall fragmentation and discussed the catastrophic mechanism of the “support-surrounding rock” system on the background of fully mechanized caving face with large inclination soft coal. Hua and Xie [8] found 12 factors of the coal wall slabs based on limit equilibrium theory. Dip mining, hydraulic support with high working resistance, speeding up the advancement of the working face, strengthening the coal wall, and moving frame with pressure in time were proposed to control the coal slab. Ning [9] proposed the coal wall force analysis model and the mechanism of coal slab gangs as revealed: under the action of mining stress, the coal wall first undergoes minor flexural deformation. When the mining stress reaches the peak value, cracks occur at the upper part of the coal wall at 0.35 times the mining height, and then all the coal walls fall off. Yin et al. [10] established a mechanical model of coal wall instability with different slab trajectories in a fully mechanized caving face with high-cutting height and a mechanical model of coal slab siding with weak inclusions. In addition, a safety evaluation system for coal slab slabs was developed.

The previous research mainly focused on the working face with large height and hard coal seam. The measures to prevent coal slip were proposed on the basis of clarifying the factors influencing the instability of the coal wall. However, the physical and mechanical properties of the soft coal must be one of the most important factors inducing the coal slip. Field engineering shows that water injection into the coal seam can improve the physical and mechanical properties of coal and prevent accidents, which has been successfully applied in many coal mines [11–14]. In order to study the mechanical characteristics of soft coal after water injection, experimental research on the strength and deformation characteristics of coal with different water contents was carried out. The compression test of 8# coal of the Luling Coal Mine in Huaibei under different moisture content was carried out with TSZ10 triaxial instrument, and it was found that the cohesion and shear strength of the coal can be improved by injecting reasonable water into the coal [15]. The uniaxial and triaxial compression tests of the coal body of the Xinzhuangzi Coal Mine in Huainan under different water content conditions were also carried out. Results show that the strength and deformation characteristics of the coal are related to the water content and the strength of the coal increases after reasonable water injection [16]. Wang et al. [17] measured the angle of repose of coal particles with different particle sizes and water content. The relationship between the angle of repose and the fluidity of coal powder and the cohesion between particles was discussed. It is also found that the physical and mechanical properties of soft coal can be significantly improved after water injection, which has a positive effect on controlling the stability of coal. However, the mesomechanical mechanism of water injection to enhance coal stability is still unclear. Therefore, in the present study, the particle size distribution, point-load strength, water content, and mesostructural characteristic of

loose coal in Huainan were tested. The shear strength of coal under different water contents was tested to analyze the physical and mechanical properties of soft coal. The cementation form of coal particles and water in different water-bearing states were discussed based on the liquid bridge force theory, and the mechanical mechanism of water injection to enhance coal stability was revealed.

## 2. Sample Preparation and Test Method

*2.1. Preparation for Raw Coal.* The 7# coal seam in Huainan is a typical soft coal seam, which is rich in folds and varying in shape. The coal body with well-developed structure has much band-shaped, granular, scaly, and powder-like primary fissures. There is almost no cohesiveness in the extremely fragile coal. The cut loose coal is extremely small, with many large pores, and it is muddy (Figure 1). During the mining of the 7# coal seam, large-scale splinters and roof fall accidents occurred frequently, which seriously affected production safety. Therefore, the 7# coal in the Huainan mining area was selected in the present study [18].

### 2.2. Test Methods

*2.2.1. Particle Size Distribution.* Standard sieves with diameters of 0.10 mm, 0.25 mm, 0.45 mm, 0.65 mm, 1.25 mm, 2.50 mm, 5.00 mm, and 10.00 mm were used to separate 3 groups of coal in turn and weigh the coal in each particle size range.

*2.2.2. Point-Load Strength.* The soft raw coal cannot be made into a standard sample with a diameter of 50 mm and a height of 100 mm. Therefore, the HDH-1 (Figure 2) point-load device with a maximum loading force of 50 kN and an accuracy of 0.001 kN was used to test the point-load strength of raw coal. In order to ensure the reliability of the test, the height ( $h$ ) and width ( $b$ ) of the smallest cross section through the loading point while loading were within the range of  $40 \pm 5$  mm and  $50 \pm 5$  mm, respectively, and the sample length is 1.5 times the minimum cross-sectional height of the loading point (Figure 3).  $L$  and  $P$  in Figure 3 represent the sample length and load, respectively. The point-load strength of 15 coal blocks was tested in this study.

*2.2.3. Water Content.* Firstly, weigh 10 coal blocks weighing more than 50 g and then dry them at  $105^{\circ}\text{C} \sim 110^{\circ}\text{C}$  for 24 hours. Secondly, cool the 10 coal blocks and weigh them again.

*2.2.4. Mesostructural Characteristic.* A coal block with a relatively flat surface and a size of  $5 \text{ mm} \times 5 \text{ mm} \times 10 \text{ mm}$  is used to observe the surface image by S-3000N scanning electron microscope.

*2.2.5. Shear Strength of Coal with Different Water Contents.* The dry raw coal was fully crushed and then sieved with standard soil sieves to screen out the coal with a particle size

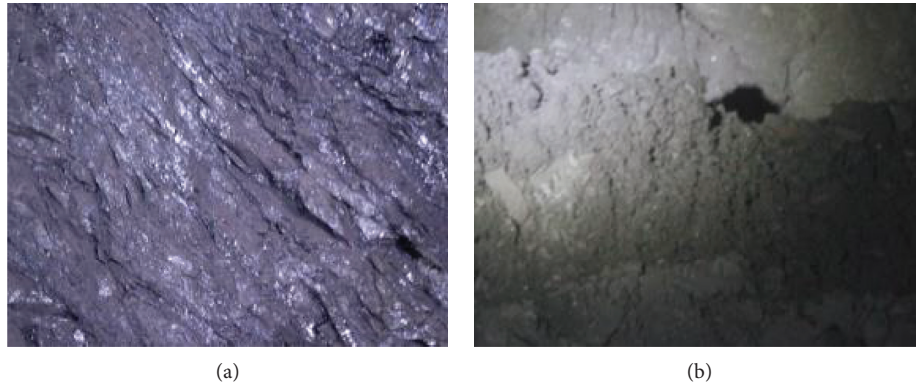


FIGURE 1: State of coal seam: (a) coal wall; (b) dropped loose coal.



FIGURE 2: Point-load device.

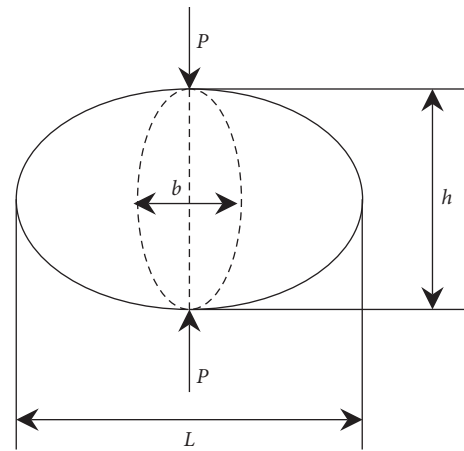


FIGURE 3: Sample loading diagram.



FIGURE 4: STSJ-5 smart electric quadruple direct shear apparatus.

of 0.10~0.25 mm. Eight kinds of coal samples with different water contents were prepared by mixing the same weight of coal particles and different weight of water. There are 4 coal samples with the same moisture content.

The STSJ-5 smart electric quadruple direct shear apparatus (Figure 4) was used to test the shear strength of coal. The shear rate is 0.02 mm/min, and the normal stress was set to 50 kPa, 100 kPa, 200 kPa, and 400 kPa in turn for coal samples with the same water content. The reading of dynamometer was recorded in real time during the test. The broken coal sample was collected after the test, the actual water content of the coal sample was measured, and the average water content of the same sample was used as the effective experimental data.

### 2.3. Data Analysis Method

2.3.1. *Fractal Dimension of Coal Particle Size.* According to the fractional fractal theory, the fractal dimension ( $D$ ) [19] of coal particle size can be defined as

$$D = 3 - a, \tag{1}$$

where  $a$  is the slope of  $(M_R/M \times 100, R)$  in double logarithmic coordinates,  $M_R$  is the cumulative weight of fragments with a particle size smaller than  $R$ , g;  $M$  is the total weight of coal, g.

2.3.2. *Point-Load Strength* [20]. The point-load index ( $I_s$ ) can be defined as follows:

$$I_s = \frac{\pi P_{\max}}{4hb}, \quad (2)$$

where  $P_{\max}$  is the peak load, N.

The point-load index of irregular specimens can be corrected as follows:

$$I_{s(50)} = I_s \left( \frac{\sqrt{4hb/\pi}}{50} \right)^{0.45}. \quad (3)$$

The uniaxial compressive strength ( $R_c$ ) of coal can be written as follows:

$$R_c = 19I_{s(50)}. \quad (4)$$

The uniaxial tensile strength ( $R_t$ ) of coal can be written as follows:

$$R_t = 0.82I_{s(50)}. \quad (5)$$

2.3.3. *Shear Strength*. The shear strength ( $S$ ) of coal can be given as follows:

$$S = C \times R_t, \quad (6)$$

where  $C$  is the coefficient of force measuring ring, 1.499 kPa/0.01 mm, and  $R_t$  is the peak reading of dynamometer, 0.01 mm. Taking the normal pressure ( $p$ ) and shear strength ( $S$ ) of the same moisture content sample as the abscissa and ordinate, respectively, the linear fit line was then drawn on the coordinate axis based on different ( $p$ ,  $S$ ). The internal friction angle and cohesion can be represented by the inclination of the fitted straight line and the intercept of the line on the vertical axis, respectively.

### 3. Test Results

#### 3.1. Physical and Mechanical Properties of Raw Coal

3.1.1. *Particle Size Distribution*. The content of coal particles with different sizes is different (Table 1 and Figure 5). Among them, the content of coal particles in the range of 2.5~5 mm is the largest, which is 31.18%, followed by the particle coal with a particle size of 5~10 mm, which is 21.66%, and the content of coal particles smaller than 0.1 mm is the smallest, which is 1.61%. Generally speaking, the content of coal particles increases with the increase in particle size in the test range. The broken coal contains a lot of fine particles. The content of coal particles with a particle size of less than 2.5 mm is 47.16%. The fractal dimensions of the particle size of the three groups of samples are 2.188, 2.324, and 2.004, respectively, with an average value of 2.172.

3.1.2. *Point-Load Strength*. The uniaxial compressive and tensile strengths of raw coal are quite small, with the minimum values of 2.204 MPa and 0.095 MPa, respectively, the maximum values of 7.600 MPa and 0.328 MPa,

respectively, and the average values 3.822 MPa and 0.165 MPa, respectively (Table 2).

3.1.3. *Water Content*. The maximum water content of raw coal is 1.619%, the minimum is 1.131%, and the average is 1.336% (Table 3).

3.1.4. *Mesostructural Characteristic*. It can be seen in Figure 6 that the outline of the clot-like particles in the coal is low in definition, and the edges and corners are not obvious. The loose particles with weak cohesion are mainly in point-to-point contact. The internal pores and fissures of the coal are fully developed, large in volume and large in number, and the distribution density is high. The intergranular pores and fissures are the main ones, and the intragranular pores and fissures are few.

On the whole, there are initial defects of different shapes and sizes in the coal body. The distribution of particles, pores, and cracks is uneven and discontinuous, and it contains a large number of loose clusters and flocculent structures. There are a large number of loose particles, pores, and cracks. The raw coal has the apparent characteristics of high porosity.

In summary, the raw coal is dry and has extremely low macrostrength and a highly porous mesostructure, which is the essential cause of easy instability.

#### 3.2. Shear Strength of Coal with Different Water Contents.

Figure 7 shows the shear stress-displacement curve of extremely soft coal with different water contents. It can be seen that when  $w = 0.966\%$ , as the displacement increases, the shear stress gradually increases and then decreases significantly after reaching the peak. The softening characteristics of coal samples under various normal stresses are obvious, and they have certain brittle failure characteristics. The coal sample with a water content of 3.841% has certain softening characteristics when the normal stress is 50 kPa or 100 kPa. However, when the normal stress is 200 kPa or 400 kPa, as the displacement increases, the shear stress increases slowly and then tends to a progressive value, and the shear stress has no obvious peak value. The hardening characteristics and ductile failure characteristics of the coal specimens gradually became prominent. For a coal sample with a water content of 7.688%, the shear stress-displacement curve shows softening characteristics when the normal pressure is 50 kPa and shows obvious hardening characteristics when the normal pressure is 100 kPa, 200 kPa, or 400 kPa. The shear stress-displacement curves of coal specimens under different normal stresses all have certain hardening characteristics when the water content reaches 12.957%, 17.888%, 20.847%, 22.072%, or 24.526%. In general, with the increase of water content and normal pressure, the shear stress-displacement curve gradually transforms from softening to hardening type, and the failure type slowly transitions from brittleness to ductility.

The shear strength of coal under different water contents increases with the increase of normal pressure (Table 4). The

TABLE 1: Particle size distribution of raw coal.

Number	Particle size (mm)	Particle size distribution								$\alpha$	$D$
		<0.1	0.1~0.25	0.25~0.45	0.45~0.65	0.65~1.25	1.25~2.5	2.5~5	5~10		
A1	Weight (g)	5.39	23.97	15.4273	18.63	48.89	20.78	115.99	59.72	0.812	2.188
	Percentage	1.75	7.76	4.99	6.03	15.83	6.73	37.57	19.34		
A2	Weight (g)	8.23	56.66	25.17	24.91	55.75	20.26	73.64	61.62	0.676	2.324
	Percentage	2.52	17.37	7.72	7.64	17.09	6.21	22.57	18.89		
A3	Weight (g)	2.03	28.84	19.21	20.30	50.90	22.53	120.59	96.61	0.996	2.004
	Percentage	0.563	7.990	5.321	5.624	14.099	6.240	33.403	26.760		
Average	Percentage	1.61	11.04	6.01	6.43	15.67	6.39	31.18	21.66		2.172

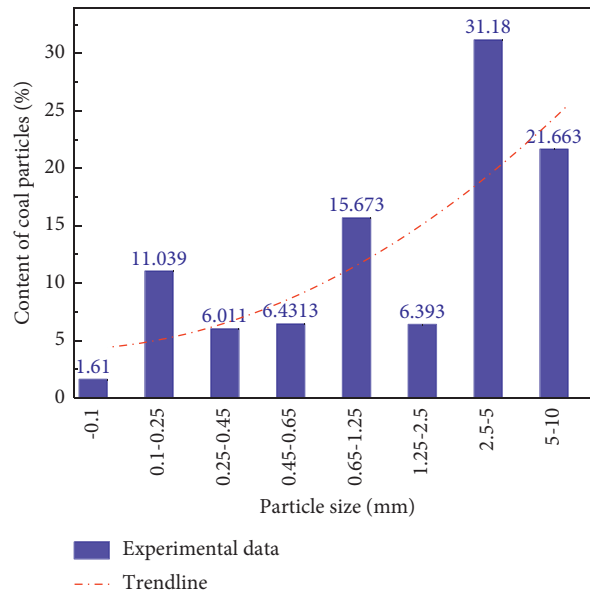


FIGURE 5: Particle size distribution of raw coal.

TABLE 2: Point-load strength of coal.

Number	$h$ (mm)	$b$ (mm)	$P_{\max}$ (N)	$I_{s(50)}$ (MPa)	$R_c$ (MPa)	$R_t$ (MPa)
B1	37.9	53.1	403	0.158	3.002	0.130
B2	47.2	56.0	504	0.160	3.040	0.131
B3	45.8	60.8	609	0.186	3.534	0.153
B4	39.1	53.4	785	0.299	5.681	0.245
B5	44.2	49.7	1090	0.400	7.600	0.328
B6	48.7	50.6	688	0.231	4.389	0.189
B7	40.9	68.2	512	0.156	2.964	0.128
B8	47.6	57.0	453	0.141	2.679	0.116
B9	50.7	62.8	421	0.116	2.204	0.095
B10	38.2	47.9	411	0.174	3.306	0.143
B11	43.0	58.0	541	0.18	3.420	0.148
B12	39.6	62.2	646	0.217	4.123	0.178
B13	44.4	47.4	497	0.188	3.572	0.154
B14	49.0	55.3	452	0.141	2.679	0.116
B15	46.6	59.9	887	0.270	5.130	0.221
Average					3.822	0.165

internal friction angle of the coal does not change significantly with the water content, being within the range of  $12.54^\circ \sim 14.72^\circ$ . However, as the water content increases, the

cohesion of coal first increases and then decreases (Figure 8). When the water content is 0.966%, the cohesion of coal is the smallest, which is 1.89 kPa, and when the water content is

TABLE 3: Water content of raw coal.

Number	Coal weight (g)	Dried coal weight (g)	Water content (%)
C1	87.886	86.903	1.131
C2	115.471	114.047	1.249
C3	82.653	81.453	1.473
C4	188.332	185.505	1.524
C5	225.326	222.018	1.490
C6	151.889	150.132	1.170
C7	266.337	262.093	1.619
C8	98.333	96.992	1.383
C9	178.008	176.005	1.138
C10	136.711	135.116	1.180
Average			1.336

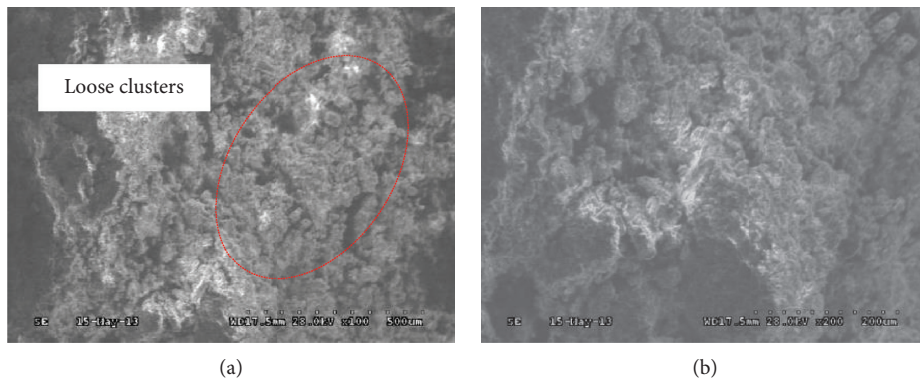


FIGURE 6: SEM picture of coal body: (a) 100 times; (b) 200 times.

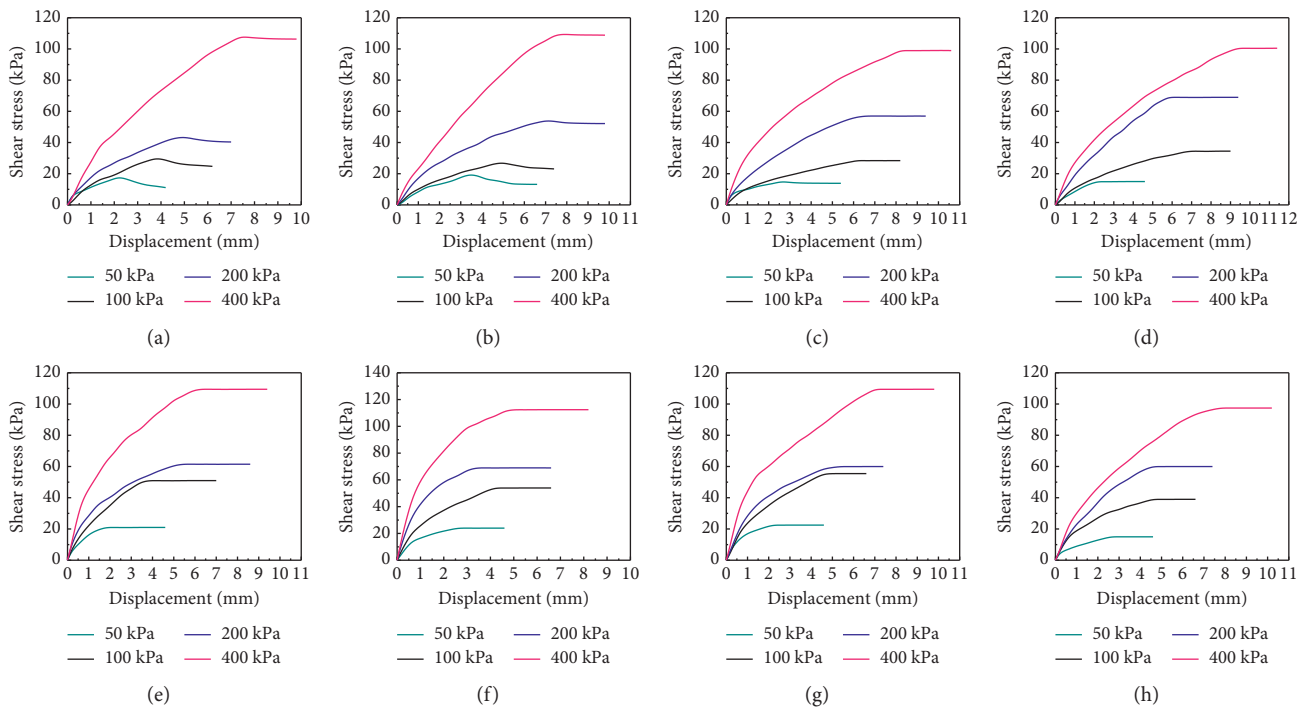


FIGURE 7: Shear stress-displacement curve of extremely soft coal: (a)  $w = 0.966\%$ ; (b)  $w = 3.841\%$ ; (c)  $w = 7.688\%$ ; (d)  $w = 12.957\%$ ; (e)  $w = 17.888\%$ ; (f)  $w = 20.847\%$ ; (g)  $w = 22.072\%$ ; (h)  $w = 24.526\%$ .

TABLE 4: Coal shear strength index under different water contents.

Number	$w$ (%)	$p$ (kPa)	$S$ (kPa)	$c$ (kPa)	$\varphi$ (°)
D11	0.966	50	17.988	1.89	14.34
D12		100	29.98		
D14		150	43.471		
D14		200	107.928		
D21	3.841	50	19.487	3.1935	14.72
D22		100	26.982		
D24		150	53.964		
D24		200	109.427		
D31	7.688	50	14.99	5.0184	13.45
D32		100	28.481		
D34		150	56.962		
D34		200	98.934		
D41	12.957	50	14.99	10.037	13.4
D42		100	34.477		
D44		150	68.954		
D44		200	100.433		
D51	17.888	50	20.986	17.206	13.06
D52		100	50.966		
D54		150	61.459		
D54		200	109.427		
D61	20.847	50	23.984	21.182	13.11
D62		100	53.964		
D64		150	68.954		
D64		200	112.425		
D71	22.072	50	22.485	19.943	12.59
D72		100	55.463		
D73		150	59.96		
D74		200	109.427		
D81	24.526	50	14.99	11.145	12.54
D82		100	38.974		
D83		150	59.96		
D84		200	97.435		

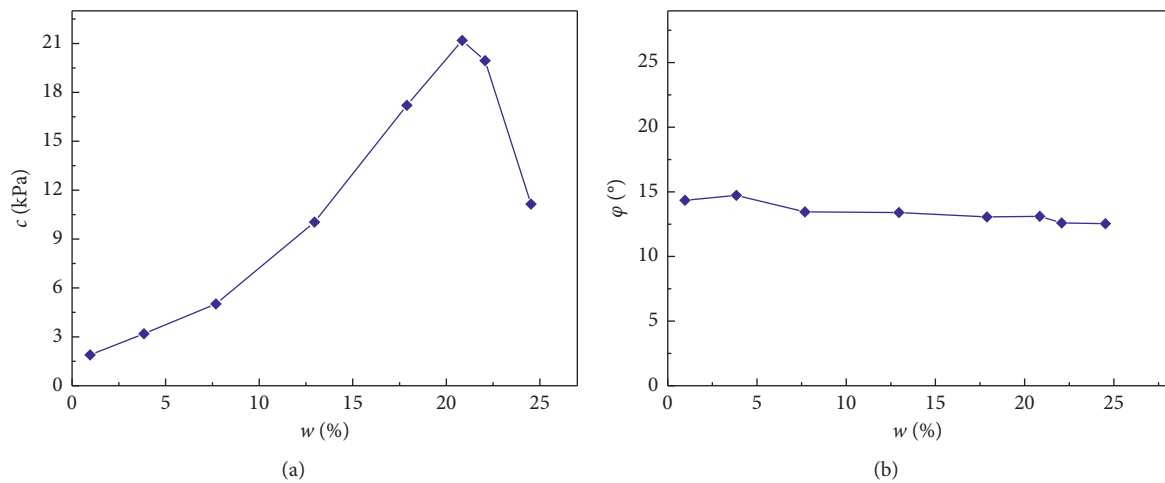


FIGURE 8: Cohesion (a) and internal friction angle (b) of coal under different water contents.

20.847%, the cohesion of coal reaches the maximum of 21.182 kPa. Therefore, reasonable water injection can significantly enhance the strength of coal.

#### 4. Discussion

The force inside the coal body after water injection mainly includes two parts: one is the cohesion between particles, and the other is the liquid bridge force generated from the liquid bridge formed by particles and water [21]. The liquid bridge force is caused by capillary pressure, surface tension, and viscous force. There is no obvious change in the cohesiveness of coal under different water contents. The change of the liquid bridge force with the water content is the main reason for the evolution of the macromechanical characteristics of coal. Therefore, it is necessary to clarify the shape of the liquid bridge and the change law of the liquid bridge force inside the coal body to reveal the mechanical mechanism of water injection modification to increase the stability of the coal body. The liquid bridge force can be characterized by the liquid saturation ( $s$ ) as follows:

$$s = \frac{V_L}{V_T} \times 100\%, \quad (7)$$

where  $V_L$  is the volume of water,  $\text{cm}^3$ , and  $V_T$  is the pore volume of coal,  $\text{cm}^3$ .

The liquid saturation is determined by water content ( $w$ ) and pores of coal. The water content of coal can be defined as follows:

$$w = \left( \frac{M_1}{M_2} - 1 \right) \times 100\%, \quad (8)$$

where  $M_1$  is the weight of raw coal, g, and  $M_2$  is the weight of dried coal, g. The water content of coal can be further given as follows:

$$w = \frac{M_L}{\rho_2 V} \times 100\%, \quad (9)$$

where  $M_L$  is the weight of water in the coal, g;  $\rho_2$  is the density of dried coal,  $\text{g}/\text{cm}^3$ ; and  $V$  is the volume of coal,  $\text{cm}^3$ . Therefore, the volume of water can be written as follows:

$$V_L = \frac{w \rho_2 V}{\rho_1}, \quad (10)$$

where  $\rho_1$  is the density of water,  $1 \text{ g}/\text{cm}^3$ .

The porosity of coal ( $n$ ) can be given as follows:

$$n = \frac{V_T}{V} \times 100\%. \quad (11)$$

Combining (7)–(12), the liquid saturation can be deduced as follows:

$$s = \frac{w \rho_2}{\rho_1 n} \times 100\%. \quad (12)$$

It can be found that the liquid saturation increases in direct proportion with the water content of the coal when other conditions are the same.

It is assumed that there are two kinds of particles inside the coal: large and small particles. Based on the linear relationship between liquid saturation and water content, the change of the liquid bridge composed of coal particles and water with the water content can be divided into 4 stages (Figure 9).

Assuming that  $f_1$  is the liquid bridge force between small particles,  $f_2$  is the liquid bridge force between large particles, and  $f_{12}$  is the liquid bridge force between large and small particles, the total liquid bridge force ( $F$ ) can be written as follows:

$$F = f_1 + f_2 + f_{12}. \quad (13)$$

Table 5 shows the variation law of liquid bridge force with water content in different stages. The following can be found:

State I: the  $w$  and  $s$  values are extremely low. The liquid bridges between small particles and between large and small particles are pendulum-shaped or cord-shaped, and the liquid bridges between large particles are pendulum-shaped. With the increase of water content,  $f_1$ ,  $f_{12}$ ,  $f_2$ , and  $F$  values all increase slowly, and the macroscopic strength of the coal body increases slowly.

State II: the  $w$  and  $s$  values are quite low. The liquid bridges between small particles and between large and small particles are capillary-shaped, and the liquid bridges between large particles are cord-shaped. With the increase of water content,  $f_1$ ,  $f_{12}$ ,  $f_2$ , and  $F$  values all increase, and the macroscopic strength of the coal body increases correspondingly.

State III: the  $w$  and  $s$  values are moderate. The liquid bridges between small particles and between large and small particles are muddy, and the liquid bridges between large particles are capillary-shaped. With the increase of water content,  $f_1$ ,  $f_{12}$ ,  $f_2$ , and  $F$  values all increase, and the macroscopic strength of the coal body increases correspondingly. With the increase of water content,  $f_1$  and  $f_{12}$  gradually decrease,  $f_2$  increases significantly, and the increment of  $f_2$  is much larger than the decrease of  $f_1$  and  $f_{12}$ .  $F$  reaches the peak, the total force inside the coal body reaches the maximum value, and the macroscopic strength is the highest.

State IV: the  $w$  and  $s$  values are quite high. The liquid bridges between different particles are muddy. With the increase of water content,  $f_1$ ,  $f_{12}$ ,  $f_2$ , and  $F$  values all decrease obviously, and the macroscopic strength of the coal body decreases correspondingly.

The mechanical mechanism of water injection to enhance coal stability can be summarized as follows: the loose raw coal contains a large number of fine particles. The liquid bridge composed of soft coal particles and water is mainly capillary-shaped, the liquid bridge force reaches the maximum, and the total internal force is the strongest after reasonable water injection into the coal. Water can promote coal particles which can be agglomerated and cemented by water, causing the coal body to transform from an unstable

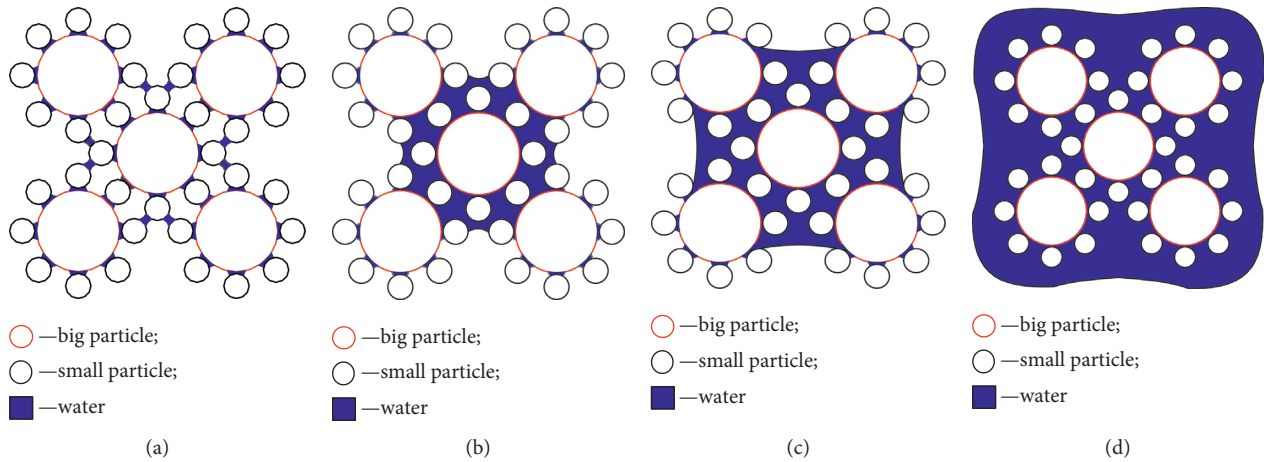


FIGURE 9: Shape of water-coal liquid bridge at different stages: (a) State I; (b) State II; (c) State III; (d) State IV.

TABLE 5: Shape of liquid bridge and variation law of liquid bridge force with water content.

State	Form of liquid bridge			$f_1$	$f_2$	$f_{12}$	$F$
	Between small particles	Between large and small particles	Between big particles				
I	Pendulum-shaped and cord-shaped	Pendulum-shaped and cord-shaped	Pendulum-shaped	↑	↑	↑	↑
II	Capillary-shaped	Capillary-shaped	Cord-shaped	↑	↑	↑	↑
III	Muddy	Muddy	Capillary-shaped	↓	↓	↓	↓
IV	Muddy	Muddy	Muddy	↓	↓	↓	↓

loose body to a stable continuum. The strength and stability of the coal body are thus improved.

### 5. Conclusions

The physical and mechanical properties of 7# coal in Huainan were analyzed, and the direct shear test of coal under different water contents was carried out. The mechanical mechanism of water injection in coal to increase its stability was discussed based on the liquid bridge force theory. The main conclusions are as follows:

- (1) The particle size distribution of the soft coal has obvious regularity, which is in the state of a loose medium and low strength. With the increase of particle size, the weight ratio of coal gradually increases. The weight percentage of particle coal with a particle size of less than 2.5 mm is 47.157%, and the fractal dimension is 2.172. The uniaxial compressive and tensile strengths of the raw coal are 3.822 MPa and 0.165 MPa, respectively.
- (2) The water content of the raw coal is 1.336%, which is relatively dry. The raw coal contains many loose clusters and flocculent structures. There are a large number of loosely arranged particles, pores, and cracks, and the raw coal shows the characteristics of high porosity, which is the essential cause of low strength, brokenness, and easy instability and disaster.
- (3) The strength and deformation characteristics of the soft coal body change obviously with the water

content. In the test water content range (0.966%~26.580%), with the increase of water content, the shear stress-displacement curve of coal gradually transforms from softening to hardening type, and the failure type transitions from brittleness to ductility slowly. The internal friction angle of the coal does not change significantly with the water content; however, the cohesion presents a trend of increasing first and then decreasing. The cohesion reaches the peak value when the moisture content is within the range of 17.888%~22.072%. Therefore, the coal body has the highest strength and the strongest stability when the water content is reasonable.

- (4) The mechanical mechanism of water injection to enhance coal stability can be summarized as follows: the liquid bridge composed of soft coal particles and water is mainly capillary-shaped, the liquid bridge force reaches the maximum, and the total internal force is the strongest after reasonable water injection into the coal. Water can promote coal particles which can be agglomerated and cemented by the water, causing the coal body to transform from an unstable loose body to a stable continuum. The strength and stability of the coal body are thus improved.

### Data Availability

The experimental results used to support the findings of this study are included within the article.

## Conflicts of Interest

The authors declare that they have no conflicts of interest.

## Acknowledgments

The authors are grateful to the National Natural Science Foundation of China (no. 52004007), the Independent Research Foundation of the State Key Laboratory of Mining Response and Disaster Prevention and Control in Deep Coal Mines (SKLMRDPC19ZZ09), and the Opening Foundation of the State Key Laboratory of Mining Response and Disaster Prevention and Control in Deep Coal Mines (Grant no. SKLMRDPC20KF09).

## References

- [1] G. Wang, Y. Pang, and J. Liu, "Determination and influence of cutting height of coal by top coal caving method with great mining height in extra thick coal seam," *Journal of China Coal Society*, vol. 37, no. 11, pp. 1777–1782, 2012.
- [2] Y. Xu, G. Wang, M. Li, Y. Xu, H. Han, and J. Zhang, "Investigation on coal face slabbed spalling features and reasonable control at the longwall face with super large cutting height and longwall top coal caving method," *Journal of China Coal Society*, vol. 46, no. 2, pp. 357–369, 2021.
- [3] Y. Pang, G. Wang, and H. Ren, "Multiple influence factor sensitivity analysis on coal wall spalling of workface with large mining height," *Journal of Mining and Safety Engineering*, vol. 36, no. 4, pp. 736–745, 2019.
- [4] X. Zhang, *Study on mechanism characteristics and application of fully mechanized top coal caving mining with great mining height in very thick coal seam*, Ph.D. thesis, Anhui University of Science and Technology, Huainan, China, 2012.
- [5] X. Li, T. Kang, Y. Yang et al., "Analysis of coal wall slip risk and caving depth based on Bishop method," *Journal of China Coal Society*, vol. 40, no. 7, pp. 1498–1504, 2015.
- [6] J. Jin, X. Meng, and Z. Gao, "Analysis on spalling depth of coal wall in large-height mining face," *Mining Research and Develop*, vol. 38, no. 5, pp. 77–79+89, 2011.
- [7] Y. Wu, D. Lang, and P. Xie, "Mechanism of disaster due to rib spalling at fully-mechanized top coal caving face in soft steeply dipping seam," *Journal of China Coal Society*, vol. 41, no. 8, pp. 1878–1884, 2016.
- [8] X. Hua and G. Xie, "Coal wall spalling mechanism and control technology of fully mechanized high cutting longwall coal mining face," *Coal Science and Technology*, vol. 36, no. 9, pp. 1–3+24, 2008.
- [9] Y. Ning, "Mechanism and control technique of the rib spalling in fully mechanized mining face with great mining height," *Coal Science and Technology*, vol. 34, no. 1, pp. 50–52, 2009.
- [10] S. Yin, F. He, and G. Cheng, "Study of criterions and safety evaluation of rib spalling in fully mechanized top-coal caving face with large mining height," *Journal of China University of Mining and Technology*, vol. 44, no. 5, pp. 800–807, 2015.
- [11] H. Han, Z. Wang, and B. Guo, "Coal wall spalling mechanism and prevention technology of unstable seam with soft roof, soft coal and soft floor," *Coal Science and Technology*, vol. 44, no. 4, pp. 34–38, 2016.
- [12] L. Chen, Y. Li, and D. Zhao, "Coal wall spalling influencing factors and countermeasures of fully mechanized longwall coal mining face," *Coal Engineering*, vol. 45, no. 10, pp. 54–56, 2013.
- [13] C. Gong, "Dynamic pressure water injection on coal wall of 2103 working face of heilong mining industry," *Coal*, vol. 28, no. 12, pp. 25–26+36, 2019.
- [14] J. Guo, Y. Zou, H. Zhou, and J. Tian, "Effect and application of water injecting technology in coal seam of Zhenxing No. 2 coal mine," *Coal Mining Technology*, vol. 23, no. 6, pp. 122–124+107, 2018.
- [15] J. Wang, "Mechanism of the rib spalling and the controlling in the very soft coal seam," *Journal of China Coal Society*, vol. 32, no. 8, pp. 785–788, 2007.
- [16] L. Wang, C. Zhu, Z. Yin, and J. Hou, "Research on soft coal mechanics characteristic test for moisture content effect," *Journal of Mining and Safety Engineering*, vol. 33, no. 6, pp. 1145–1151, 2016.
- [17] W. Wang, J. Zhang, S. Yang, H. Zhang, H. Yang, and G. Yue, "Experimental study on the angle of repose of pulverized coal," *Particuology*, vol. 8, no. 5, pp. 482–485, 2010.
- [18] L. Yang and X. Cheng, "Improving coal seam water injection effect under optimized water injection parameters and technology," *Coal Mining Technology*, vol. 21, no. 3, pp. 132–134, 2016.
- [19] M. He, G. Yang, J. Miao, X. Jia, and T. Jiang, "Classification and research methods of rockburst experimental fragments," *Chinese Journal of Rock Mechanics and Engineering*, vol. 28, no. 8, pp. 1521–1529, 2009.
- [20] J. A. Franklin, P. Pells, D. McLachlin et al., "International society for rock mechanics experimental methods committee the suggested method of determination of point load strength," *Chinese Journal of Rock Mechanics and Engineering*, vol. 5, no. 1, pp. 79–90, 1986.
- [21] Q. Sun and G. Wang, *An Introduction to the Mechanics of Granular Materials*, China Science Publishing and Media Ltd., Beijing, China, 2009.